Morphologic changes in idiopathic condylar resorption with different degrees of bone loss

Yifan He, BS,[a,#] Han Lin, DDS, PhD,[b,#] Qiuping Lin, MD,[c] Lin Lu, BS,[a] Mingyu Li, BS,[d] Qianli Li, BS,[a] Jingyi Xue, BS,[a] and Yue Xu, DDS, PhD[a]

Objective. The aim of this case control study was to investigate the sizes, shapes, and articular surface angles of condyles exhibiting idiopathic condylar resorption (ICR) with different degrees of condylar bone loss and to provide additional information for the diagnosis of ICR.

Study Design. In total, 154 condyles from patients with ICR and 42 healthy condyles were included. The ICR group was further divided into 3 subgroups (ICR I, ICR II, and ICR III) based on the morphology of the condyle. Three-dimensional (3-D) models of the condyles were measured and analyzed by using the Mimics software based on cone beam computed tomography data.

Results. The condylar anteroposterior diameter, transverse diameter, height, superficial area, volume, articular surface angles, condylar neck angle, maximal sectional area, and condylar neck sectional area were all significantly different between the ICR group and the control group ($P < .05$). There were also significant differences among the 3 subgroups in many of these parameters ($P < .05$).

Conclusions. Morphologic changes in ICR become worse as the disease progresses, with significant differences between diseased and normal condyles. There were many significant differences among the subgroups. Posteriorly inclined condylar neck and slender condylar neck may be associated with ICR. (Oral Surg Oral Med Oral Pathol Oral Radiol 2019;128:332−340)

Idiopathic condylar resorption (ICR), an irreversible disease with a low incidence,[1] is characterized by progressive and extensive condylar resorption and loss of ramus height with or without temporomandibular joint (TMJ) symptoms. If ICR is not treated in a timely manner, it can eventually bring about a series of complications, including severe malocclusion, facial malformation, and irreversible joint dysfunction.

When abnormal joint loading or sustained physical stress to the articular structures of the TMJ exceeds the normal adaptive capacity, dysfunctional remodeling changes occur in the mandible. These changes result in a series of morphologic abnormalities, such as decreased condylar volume and ramus height, progressive mandibular retrusion, or decreased mandibular growth.[2−4] A relatively rapid loss of condylar volume and decrease in height are common clinical presentations of ICR. As condylar resorption progresses in the ICR process, the mandible becomes retruded, and the mandibular plane angle and the anterior face height increase, resulting in anterior open bite or class II malocclusion.[5] Clinically, the most common initial symptom in patients with ICR is alteration of masticatory function.[6] Other clinical symptoms, such as facial deformity (e.g., skeletal class II malocclusion and mandibular deviation), or typical TMJ symptoms, such as joint clicking, pain, and limited mouth opening capacity, may also exist. In the early stage of ICR, 25% of patients may not exhibit any TMJ symptoms.[7] For this reason, early diagnosis and intervention for ICR are difficult. Moreover, because the etiology and classification of ICR are not fully understood,[8] generally accepted treatment guidelines for this disease are not available.

Historically, condylar resorption has been classified mainly on the basis of clinical manifestations. For example, Hoppenreijs divided condylar resorption into 2 types—the open bite type and the deep overbite type—and found that the risk of condylar resorption

Statement of Clinical Relevance

This study provides an important addition to the current diagnosis and classification system for idiopathic condylar resorption. The 3-dimensional morphologic changes of the condyle reflect the severity of disease. The condylar neck plays an important role in condylar resorption.

[a]Department of Orthodontics, Guanghua School of Stomatology, Hospital of Stomatology, Sun Yat-sen University, Guangdong Provincial Key Laboratory of Stomatology, Guangzhou, Guangdong, People's Republic of China.
[b]Department of Oral and Maxillofacial Surgery, Guanghua School of Stomatology, Hospital of Stomatology, Sun Yat-sen University, Guangdong Provincial Key Laboratory of Stomatology, Guangzhou, Guangdong, People's Republic of China.
[c]Department of Stomatology, Development District Hospital, Chinese Association of Medicinal Biotechnology Southern Center of Biology Diagnosis and Therapy, Guangzhou, Guangdong, People's Republic of China.
[d]Guanghua School of Stomatology, Hospital of Stomatology, Sun Yat-sen University, Guangdong Provincial Key Laboratory of Stomatology, Guangzhou, Guangdong, People's Republic of China.
Received for publication Oct 12, 2018; returned for revision May 12, 2019; accepted for publication May 30, 2019.

2212-4403/$-see front matter
https://doi.org/10.1016/j.oooo.2019.05.013
[#]co-first author.

increased with the severity of open bite.[9] With the development of radiologic technology, ICR is now mainly classified on the basis of alterations in condylar morphology. Krajenbrink et al. evaluated ICR on the basis of the condylar contour and axis by using 2-dimensional (2-D) images.[10] Gomes et al. identified different condyle types according to the similarity of the condylar surface using 3-dimensional (3-D) mesh models.[11] However, neither of these methods precisely evaluates the severity of bone loss in condylar resorption. Therefore, a strong demand exists for a more practical ICR classification as well as for a comprehensive description of the condylar morphologic characteristics of ICR.

In this study, the radiographic characteristics of ICR with different degrees of condylar bone loss were investigated by using a 3-D reconstruction technique. Morphologic analysis was performed to identify the sizes, shapes, and articular surface angles of the condyles and to propose a classification approach based on the severity of condylar bone loss.

MATERIALS AND METHODS

Patients

This study was approved by the Institutional Review Board of Sun Yat-sen University. It included 82 Chinese patients with ICR (the ICR group; mean age 30.3 ± 11.8 years) and 21 age-matched healthy controls (the control group; mean age 29.1 ± 8.5 years), who visited the Hospital of Stomatology at Sun Yat-sen University between June 2012 and June 2016. The electronic medical records of the patients with ICR were obtained from the digital database of the hospital.

Patients with ICR were included after a clinical diagnosis of ICR based on the patients' clinical records and radiographic images. The inclusion criteria were as follows[12]: (1) a history of progressive dental occlusal changes; (2) anterior open bite with at least one of the following progressive dental occlusal changes: (a) occlusal facets that cannot be approximated, or (b) changes in sequential dental occlusal measurements over time (horizontal overjet, vertical overbite, or intercuspal contacts); and (3) CT or cone beam computed tomography (CBCT) evidence of resorption of part or all of the condyle(s), or lateral cephalometric change with sequential imaging over time (clockwise mandibular rotation, i.e., increase in mandibular plane angle; increase in ANB [A point, nasion, B point]).

Patients were excluded from the study if they had rheumatologic disease, systemic joint diseases, developmental deformities, previous TMJ treatment, or a history of craniofacial surgery or trauma. Of the 82 patients with ICR, 72 had bilateral condylar involvement, and 10 had unilateral disease. All control patients were orthodontic patients with healthy TMJs, as confirmed through clinical and radiologic examinations. All control patients were selected by using the frequency matching method and were subject to the same exclusion criteria as the patients with ICR.

Radiographic examination

CBCT was performed on all of the participants, using the same unit (Vatech Co., Ltd., Hwasung, Korea). Exposure parameters were 90 kVp, 4 mA, 24 seconds, with a large field of view (at least 17 × 11 cm) including both TMJs. The CBCT images were used for both treatment planning and research. Mandibular models were reconstructed from the CBCT images and analyzed by using the interactive medical image control system Mimics 19.0 (Materialise, Leuven, Belgium).

Qualitative assessment of the condylar morphology

A total of 154 ICR condyles and 42 healthy condyles were imaged. The 3-D models of the condyles were reconstructed by using the threshold segmentation function in the Mimics software based on the gradient change of Hounsfield unit value. The anteroposterior diameter, transverse diameter, height, superficial area, and volume were measured on the 3-D models, as has been described in previous studies.[13,14] The definitions of these measurements and their associated landmarks are provided in Table I and Figure 1. First, all landmarks and planes were located on the 3-D condylar models by using the Mimics software. Then, the anteroposterior diameter, transverse diameter, and height were calculated by using the "Measure and Analyse" function as point−point distance or point−plane distance. The superficial area and volume were calculated by using the "Property" function. The articular surface angle α, articular surface angle β, and condylar neck angle γ of the condyles were measured on 2-D images, as shown in Figure 2.

Sectional area measurements

To evaluate the subtle changes in condylar shape, the ramus tangent of the condyle (a line tangent to the posterior borders of the ramus and condyle) was drawn by using the Mimics software (Figure 3). The sectional area of all the cross profiles along this tangent were created at 0.2-mm intervals.[15] The maximal sectional area (S_{max}) and the condylar neck sectional area (S_{neck}) were measured and were used to describe the shape of condyles (Figure 4).

Degrees of condylar bone loss in ICR

To further evaluate the morphologic modifications observed in ICR with different degrees of bone loss, the condyles with ICR were classified into 3 subgroups, according to the contour of the condyles (Figure 5). In the ICR I subgroup, the resorption did not reach the

Table I. Definitions of the condylar 3-dimensional (3-D) landmarks and measurements

Landmarks	*Definition*
Condylion (Co)	Superior most point of each mandibular condyle in the sagittal plane
A-point (A)	Anterior most point of each mandibular condyle in the sagittal plane
P-point (P)	Posterior most point of each mandibular condyle in the sagittal plane
M-point (M)	Interior most point of each mandibular condyle in the coronal plane
L-point (L)	Exterior most point of each mandibular condyle in the coronal plane
C-point (C)	Most caudal point of the sigmoid notch
Orbitale (Or)	Inferior most point of each infraorbital rim
Porion (Po)	Superior most point of each external acoustic meatus
Frankfort horizontal plane (FH plane)	Plane passing through the bilateral orbitale and porion points
Measurements	*Definition*
Anteroposterior diameter (A-P)	Distance between A and P
Transverse diameter (M-L)	Distance between M and L
Height (H)	Difference between the distance of Co-FH and C-FH
Superficial area (S)	Superficial area of the condyle
Volume (V)	Volume of the condyle

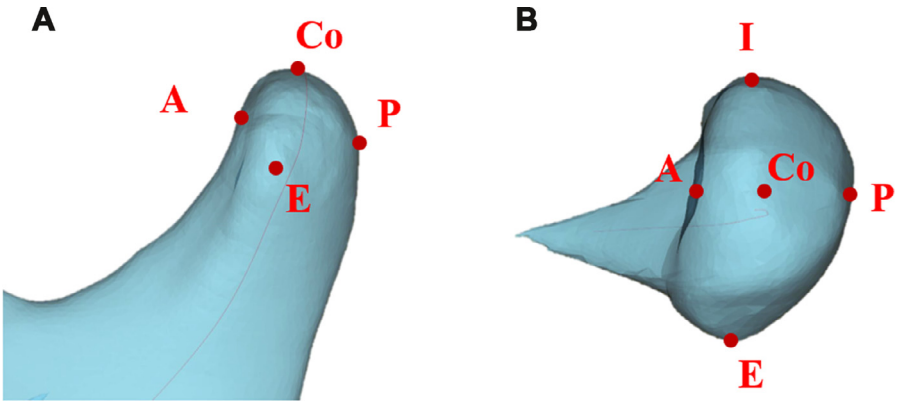

Fig. 1. The landmarks of the condyle. **A**, The landmarks of the condyle in the sagittal view. **B**, The landmarks of the condyle in the axial view. (The landmarks are defined in Table I.)

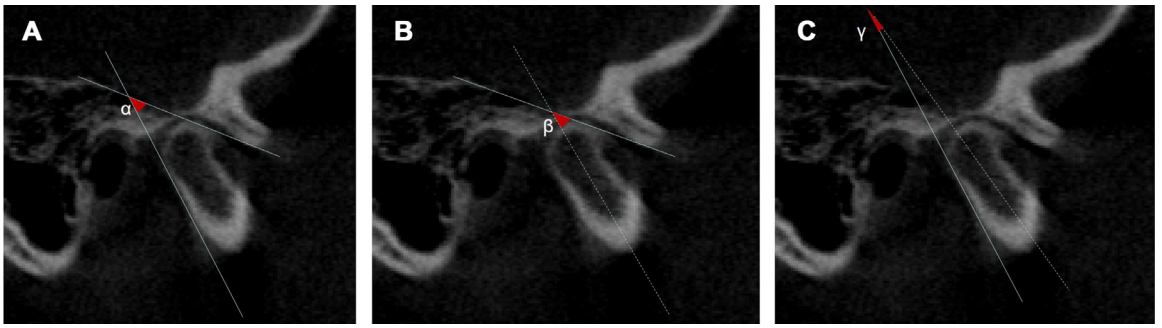

Fig. 2. Measurements of condylar morphology. **A**, Articular surface angle α: the angle of the ramus tangent and the condylar articular surface. **B**, Articular surface angle β: the angle of condylar axis and the condylar articular surface. **C**, Condylar neck angle γ: the angle of condylar axis and the ramus tangent.

maximum transverse diameter of the condyle, and both sides of the condylar lateral margins were, therefore, S-shaped. In the ICR II subgroup, the resorption transgressed the maximum transverse diameter, and both sides of the condylar lateral margins were, therefore, angular shaped. In the ICR III subgroup, the resorption was severe, causing loss of normal condylar morphology, and therefore, the contour of the sides was nearly straight. In cases where one side of the lateral margin was S-shaped and the other side was angular shaped,

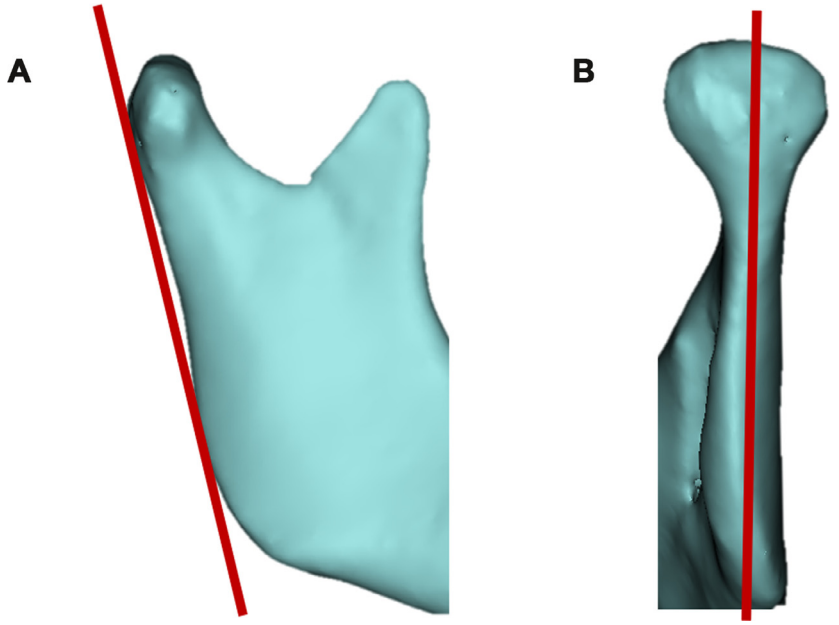

Fig. 3. The ramus tangent using Mimics software. **A**, Ramus tangent of the condyle in the sagittal view. **B**, Ramus tangent of the condyle in the coronal view.

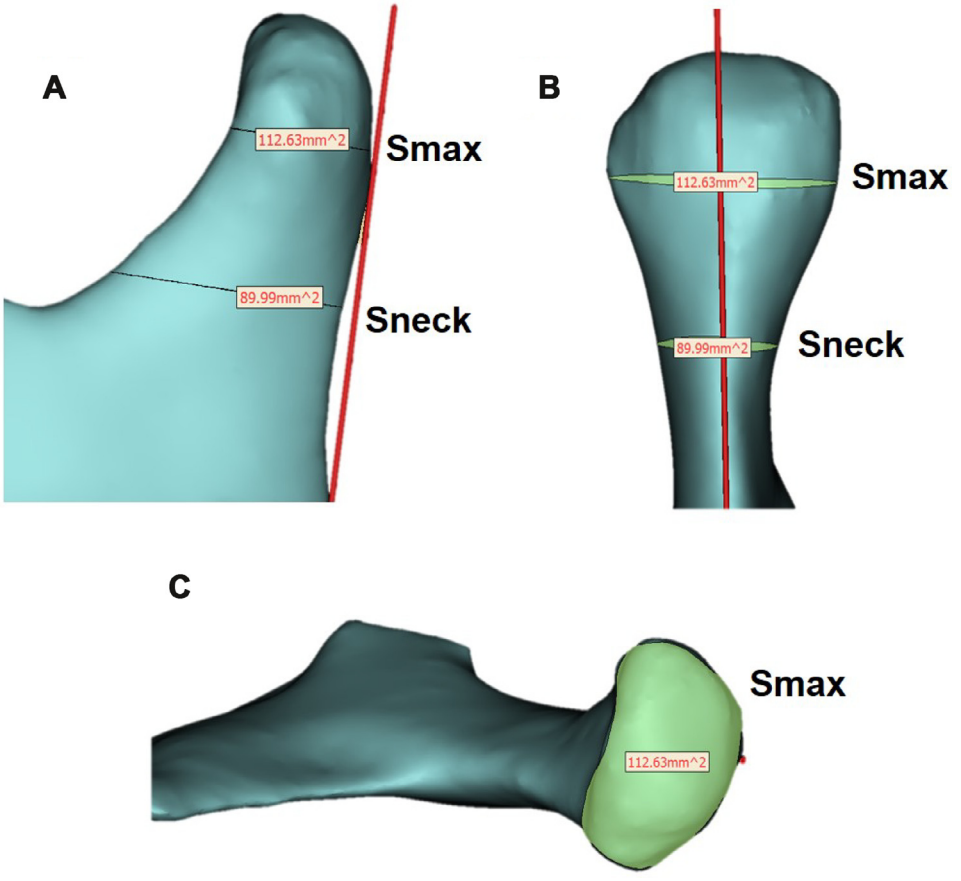

Fig. 4. Measurements of the maximal sectional area (S_{max}) and the sectional area of the condylar neck (S_{neck}) along the tangents. **A**, S_{max} and S_{neck} of the condyle in the sagittal view. **B**, S_{max} and S_{neck} of the condyle in the coronal view. **C**, S_{max} of the condyle in the axial view.

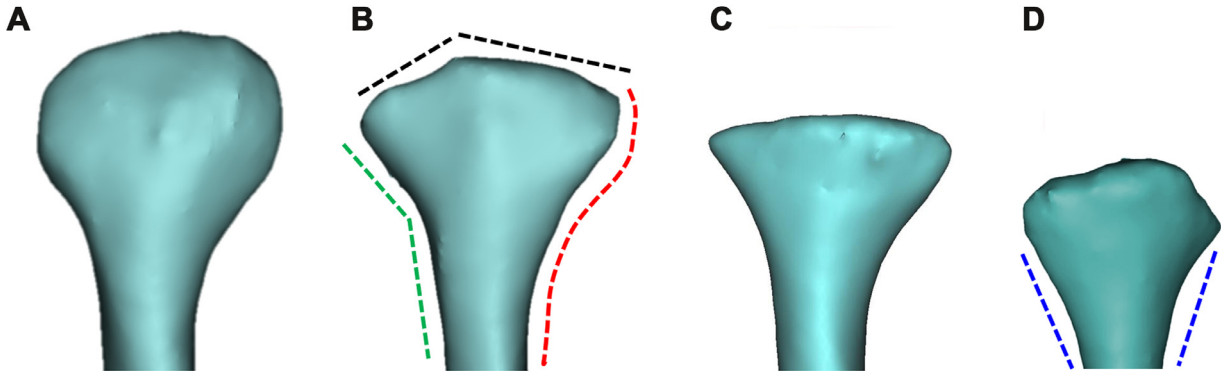

Fig. 5. Three-dimensional (3-D) modeling of idiopathic condylar resorption (ICR) subgroups. **A**, Normal condylar morphology. **B**, Condylar morphology in the ICR I subgroup. The red dotted line indicates an S-shaped lateral margin, the green dotted line indicates an angular-shaped lateral margin, and the black dotted line indicates the superior borders (the right border was larger). **C**, Condylar morphology in the ICR II subgroup. **D**, Condylar morphology in the ICR III subgroup. The blue dotted line indicates that the sides were nearly straight.

the condyle was grouped according to the side of the margin with a larger superior border. If the superior borders were equal in size, the condyle was assigned to the "more severe" subgroup.

Statistical analysis

Statistical analyses were performed with use of the SPSS software, version 20.0 (SPSS Inc., Chicago, IL). All data were expressed as mean ± standard deviation. Independent *t* tests were used to analyze the differences in measurements between the ICR group and the control group for the parameters listed in Table I. The least significant difference *t* test was used to calculate the statistical differences between all of the measurements among the subgroups (ICR I, ICR II, and ICR III). All measurements were performed by the same experienced dentist (Y.H.) and repeated at 2-week intervals. The intraclass correlation coefficients were all above 0.9, showing high reliability of the results. The average of 10 measurements was used for comparison. A *P* value less than .05 was considered statistically significant.

RESULTS

Data distribution

This study included 154 condyles from 82 consecutive patients with ICR and 42 condyles from 21 control patients. In the ICR group, mean age was 30.3 ± 11.8 years, and the male-to-female ratio was 7:75. In the control group, mean age was 29.1 ± 8.5 years, and the male-to-female ratio was 2:19. Most of the patients were females in both the ICR and control groups (Table II). There were no significant differences with regard to age or sex between the 2 groups. Of the 154 condyles in the ICR group, 61 were assigned to the ICR I subgroup, 71 to the ICR II subgroup, and 22 to the ICR III subgroup.

Table II. Characteristics of the study population

Characteristics	*ICR group*	*Control group*
Condyles	154	42
Patients	82	21
Female (%)	75 (91.46%)	19 (90.48%)
Male (%)	7 (8.54%)	2 (9.52%)
Age (years, mean ± SD)	30.3 ± 11.8	29.1 ± 8.5

ICR, idiopathic condylar resorption; SD, standard deviation.

Condylar morphology of patients with ICR

Quantitative assessments of the condylar size, shape, and articular surface angles were conducted. The anteroposterior diameter, transverse diameter, height, superficial area, and volume were significantly smaller in the ICR group compared with the control group ($P < .001$; Table III). Articular surface angle α and articular surface angle β were higher in the ICR group compared with those in the control group ($P = .007$ and $P = .022$, respectively; Table IV). The condylar neck angle was significantly larger in all 3 subgroups than in the control group ($P < .05$; Table V). S_{max} and S_{neck} were significantly smaller in the ICR I, II, and III subgroups compared with those in the control group ($P < .001$; Table V), with the average area values getting progressively lower from subgroup I through subgroup III.

Condylar morphology of the 3 ICR subgroups

The images of condyles of different groups are shown in Figure 6. The condylar volume was significantly lower in the ICR II and ICR III subgroups than in the control group ($P < .001$; Table III). All other measurements were significantly different between the ICR I, II, and III subgroups and the control group. The anteroposterior diameter, transverse diameter, height, and superficial area were significantly reduced ($P < .05$; Table III). The articular surface angles α and β were significantly increased ($P < .001$; Table IV).

Table III. Measurements of the condylar shapes and sizes in the control group, idiopathic condylar resorption (ICR) group, and different subgroups

Groups	*Anteroposterior diameter (mm)*	*Transverse diameter (mm)*	*Height (mm)*	*Superficial area (mm^2)*	*Volume (mm^3)*
Control group	8.87 ± 1.16	18.86 ± 1.85	18.47 ± 3.74	1305.66 ± 264.71	1139.70 ± 468.62
ICR group	7.14 ± 1.71*	16.91 ± 2.54*	14.79 ± 3.18*	818.31 ± 299.61*	798.80 ± 350.76*
ICR I subgroup	7.36 ± 1.67*	17.71 ± 2.26*	16.33 ± 2.73*	996.95 ± 282.34*	1013.44 ± 374.77
ICR II subgroup	7.29 ± 1.63*	17.00 ± 2.22*	14.62 ± 2.67*,†	770.15 ± 232.31*,†	731.62 ± 233.83*,†
ICR III subgroup	6.05 ± 1.71*,†,‡	14.34 ± 2.71*,†,‡	11.11 ± 2.72*,†,‡	478.43 ± 157.46*,†,‡	420.45 ± 117.48*,†,‡

*$P < .05$ vs control group.
†$P < .05$ vs ICR I subgroup.
‡$P < .05$ vs ICR II subgroup.

Table IV. Measurements of the articular surface angles in the control group, idiopathic condylar resorption (ICR) group, and different subgroups

Groups	*Articular surface angle α (°)*	*Articular surface angle β (°)*
Control group	40.04 ± 1.40	39.83 ± 1.70
ICR group	47.23 ± 4.04*	45.28 ± 3.19*
ICR I subgroup	42.86 ± 1.23*	42.25 ± 1.96*
ICR II subgroup	49.80 ± 2.56*,†	47.10 ± 2.04*,†
ICR III subgroup	50.58 ± 2.15*,†	47.78 ± 2.23*,†

*$P < .05$ vs control group.
†$P < .05$ vs ICR I group.

Table V. Measurements of the condylar neck angles, maximal sectional areas, and condylar neck sectional areas in the control group and different idiopathic condylar resorption (ICR) subgroups

Groups	*Condylar neck angle γ (°)*	*S_{max} (mm^2)*	*S_{neck} (mm^2)*
Control group	7.79 ± 1.49	134.03 ± 16.01	84.44 ± 11.43
ICR I subgroup	8.78 ± 1.32*	107.58 ± 15.18*	68.49 ± 8.87*
ICR II subgroup	9.87 ± 1.58*,†	102.35 ± 13.85*	64.69 ± 8.71*,†
ICR III subgroup	11.65 ± 0.91*,†,‡	71.57 ± 17.76*,†,‡	52.94 ± 11.55*,†,‡

*$P < .05$ vs control group.
†$P < .05$ vs ICR I group.
‡$P < .05$ vs ICR II group.

The least significant difference t-tests were performed to compare the values of the 3 ICR subgroups. Tables III and IV show the measurements describing the morphologic changes of the condylar head. The anteroposterior diameter and transverse diameter in the ICR III subgroup were significantly lower than those in the ICR I and II subgroups ($P \leq .001$). Condylar height, superficial area, and volume were significantly decreased when comparing each subgroup (I vs II, I vs III, and II vs III; $P \leq .001$; Table III). The articular surface angles α and β were significantly increased in the ICR II and ICR III subgroups compared with those in the ICR I subgroup ($P < .001$). However, there were no significant differences in these measurements between the ICR II and ICR III subgroups ($P_\alpha = 0.266$ and $P_\beta = 0.164$, respectively; Table IV).

Measurements of the condylar neck in the ICR subgroups

Condylar neck angle γ was significantly different among the subgroups (I vs II, I vs III, and II vs III; $P \leq .001$; Table V), with the average angle size becoming progressively larger from subgroup I through III. The differences in the mean articular surface angles α and β were largest between the ICR I and II subgroups ($\alpha_{I-II} = 6.94^\circ$, $\beta_{I-II} = 4.85^\circ$), followed by those between the control group and the ICR I subgroup ($\alpha_{c-I} = 2.82^\circ$, $\beta_{c-I} = 2.42^\circ$), and between the ICR II and III subgroups ($\alpha_{II-III} = 0.78^\circ$, $\beta_{II-III} = 0.68^\circ$).

The average area values of S_{max} and S_{neck} became progressively smaller from subgroup I through subgroup III. S_{max} was significantly lower in the ICR III subgroup than in the ICR I and II subgroups ($P < .001$), whereas S_{neck} was significantly decreased when comparing the subgroups (I vs II, I vs III, and II vs III; $P < .05$; Table V).

DISCUSSION

In the present study, we found that the morphologic features of the condyle differed significantly, depending on the severity of condylar bone loss in ICR, and this may provide additional information to aid in ICR diagnosis.

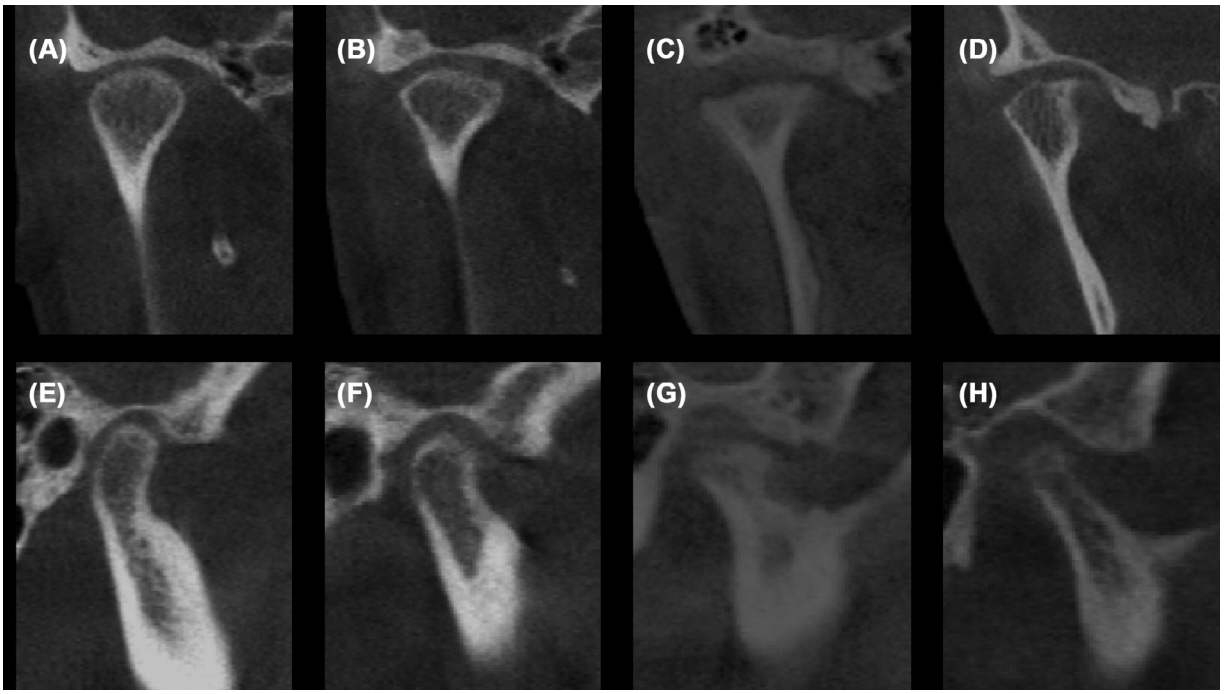

Fig 6. Cone beam computed tomography (CBCT) images in the control group and the idiopathic condylar resorption (ICR) subgroups. Coronal view of CBCT images of the condyle in the control group **(A)**, ICR I **(B)**, II **(C)**, III **(D)** subgroups. Sagittal view of CBCT images of the condyle in the control group **(E)** and the ICR I **(F)**, II **(G)**, and III **(H)** subgroups.

In this study, the subgroups of ICR represented different degrees of condylar bone loss. ICR I included cases of relatively mild resorption, in which the maximum transverse diameter of the condyle was not affected by the resorptive pattern; ICR II represented cases of moderate resorption, which transgressed the maximum transverse diameter; and ICR III was the most severe type of resorption, in which the condylar head showed alteration of normal morphology. Because ICR is generally known to be an irreversible disease, the significant differences in the measurements from these 3 ICR subgroups suggest that the condylar sizes, shapes, and angles are progressively altered in the development of ICR.

Our results showed that articular surface angle α and articular surface angle β were significantly larger in the ICR condyles than in the healthy ones. This finding may be explained by the downward and backward movement of the condylion (Co-point) after the flattening of the anterior surface. These results are consistent with previous studies that found that anterior surface flattening is one of the features of ICR.[16,17] Moreover, the articular surface angles were significantly larger in the ICR II and III subgroups than in the ICR I subgroup, whereas there was no significant difference between the ICR II and ICR III subgroups. This suggests that the changes in the anterior surface mainly occur during ICR stages I and II. In addition, the difference in the mean values of the articular surface angles α and β was largest between the ICR I and II subgroups, followed by the difference between the healthy control group and the ICR II subgroup, and between the ICR II and III subgroups. These findings suggest that the flattening of the anterior surface begins at ICR stage I, accelerates in the next stage, and becomes stable after ICR stage II. This is consistent with the findings of previous studies.[2,18,19]

In the present study, the anteroposterior diameter, transverse diameter, and height of the condyles were significantly smaller in the ICR condyles than in the healthy ones, suggesting that resorption occurs in the vertical, sagittal, and horizontal directions. This finding is consistent with previous reports. It has been reported that vertical resorption, such as severe flattening of the anterosuperior surface, commonly occurs in ICR, whereas resorption on the superior and posterior surfaces occurs simultaneously.[16,20,21] The superficial area and condylar volume also decreased in patients with ICR, suggesting that the condyles with ICR are reduced in size. This finding is consistent with the findings of previous studies.[22,23] Furthermore, we found that the anteroposterior diameter, transverse diameter, height, superficial area, and volume decreased progressively in the 3 subgroups. These findings suggest that the condylar size becomes smaller with increasing severity of bone loss in ICR. Moreover, ICR III may not be a relatively stable phase. The disease involves lysis and repair, in which more lysis may occur over time.

This suggests that morphologic changes in the condyle may become even worse than were observed in the ICR III subgroup in this investigation.

In this study, we found that the condylar neck angle γ progressively enlarged as the severity of bone loss increased. Condylar neck angle change and mandibular ramus tangent change result from the posterior rotational growth of the mandible, with seating of the reduced condyle and remodeling of the ramus being responses to the altered biomechanical status. The transformation of the upper and superior parts of the condylar head may result in posterior rotation of the mandible and, therefore, an increase in the condylar neck angle. In addition, a posteriorly inclined condylar neck may, in turn, result in excessive mechanical loading of the condylar tissues, thus causing further resorption.[14,24] The posterior tangent of the condyle was used to evaluate the condylar neck angle as the reference line because it was relatively stable throughout the progressive stages of ICR and has previously been used to identify the inclination of the condylar neck.[25] Additionally, we found a tendency toward a reduction in the sectional area of the condylar neck as the condylar resorption severity increased. The reason for this is that condylar bone remodeling occurs after condylar height reduction, recortication, and seating in the fossa and is an expected result of ICR. These results suggest that the condylar neck also plays an important role in the development of ICR.

Because of lack of long-term follow-up, the long-term changes in condylar morphology during the development of ICR could not be explored. Despite this limitation, we identified the association between the condylar shape and the severity of condylar resorption by using Mimics software. Further clinical studies are required to validate our findings.

CONCLUSIONS

This report describes the morphologic characteristics of ICR and 3 subgroups: ICR I, ICR II, and ICR III. ICR I is the initial phase of ICR, in which flattening of the anterior surface is observed, characterized by "S" shaped lateral margins. ICR II is the phase in which this flattening accelerates and angular-shaped lateral margins are observed. ICR III is characterized by severe condylar resorption, but flattening of the anterior surface, which progresses through ICR I and II, becomes relatively stable in ICR III. The anteroposterior diameter, transverse diameter, height, superficial area, and volume are related to the severity of bone loss in ICR, and they decrease progressively as the severity of ICR increases. Articular surface angles were found to progressively increase with disease severity and were significantly different from the measurements in the control condyles. The maximum transverse area of the condylar head was significantly smaller in ICR than in the control condyles. A posteriorly inclined condylar neck is associated with idiopathic condylar resorption, and an increasingly slender condylar neck is an expected result of ICR. The findings of this study provide important information that could be used to improve the current diagnosis and classification system for ICR and to deepen the understanding of the development of ICR.

DISCLOSURE

This report was funded by the National Natural Science Foundation of China (CN) (81771124, 81571020).

REFERENCES

1. Handelman CS, Mercuri L. Idiopathic/progressive condylar resorption: an orthodontic perspective. *Semin Orthodont*. 2013;19:55-70.
2. Papadaki ME, Tayebaty F, Kaban LB, Troulis MJ. Condylar Resorption. *Oral Maxillofac Surg Clin North Am*. 2007;19:223-234.
3. Mercuri LG. Osteoarthritis, osteoarthrosis, and idiopathic condylar resorption. *Oral Maxillofac Surg Clin North Am*. 2008;20:169-183.
4. Arnett GW, Milam SB, Gottesman L. Progressive mandibular retrusion—idiopathic condylar resorption. Part I. *Am J Orthodont Dentofac Orthoped*. 1996;110:8-15.
5. Arnett GW, Milam SB, Gottesman L. Progressive mandibular retrusion—idiopathic condylar resorption. Part II. *Am J Orthodont Dentofac Orthoped*. 1996;110:117-127.
6. Chouinard AF, Kaban LB, Peacock ZS. Acquired abnormalities of the temporomandibular joint. *Oral Maxillofac Surg Clin North Am*. 2018;30:83-96.
7. Mehra P, Nadershah M, Chigurupati R. Is alloplastic temporomandibular joint reconstruction a viable option in the surgical management of adult patients with idiopathic condylar resorption? *J Oral Maxillofac Surg*. 2016;74. S0278239116301124.
8. Mitsimponas K, Mehmet S, Kennedy R, Shakib K. Idiopathic condylar resorption. *Br J Oral Maxillofac Surg*. 2018;56:249-255.
9. Hoppenreijs TJM, Freihofer HPM, Stoelinga PJW, Tuinzing DB, Hof MAVT. Condylar remodelling and resorption after Le Fort I and bimaxillary osteotomies in patients with anterior open bite: a clinical and radiological study aesthetic and reconstructive surgery. *Int J Oral Maxillofac Surg*. 1998;27:81-91.
10. Krajenbrink TGA. The silhouette of the mandibular condyle on radiographs. Groningen, The Netherlands: Rijksuniversiteit te Groningen; 1994.
11. Gomes LR, Gomes M, Jung B, et al. Diagnostic index of 3 D osteoarthritic changes in TMJ condylar morphology. *Proc SPIE Int Soc Optical Engineering*. 2015: 9414.
12. Peck CC GJ, Lobbezoo F, et al. Expanding the taxonomy of the Diagnostic Criteria for Temporomandibular Disorders (DC/TMD). *J Oral Rehabil*. 2014;41:2-23.
13. Xi T, Schreurs R, Van Loon B, et al. 3 D analysis of condylar remodelling and skeletal relapse following bilateral sagittal split advancement osteotomies. *J Cranio-Maxillofac Surg*. 2015;43:462-468.
14. Kristensen KD, Schmidt B, Stoustrup P, Pedersen TK. Idiopathic condylar resorptions: 3-dimensional condylar bony deformation, signs and symptoms. *Am J Orthodont Dentofac Orthoped*. 2017;152:214-223.

15. Theopold J, Pieroh P, Scharge ML, et al. Improved accuracy of K-wire positioning into the glenoid vault by intraoperative 3 D image intensifier-based navigation for the glenoid component in shoulder arthroplasty. *Orthopaed Traumatol-Surg Res*. 2016;102: 575-581.
16. Young AL. Idiopathic condylar resorption: the current understanding in diagnosis and treatment. *J Indian Prosthodont Soc*. 2017;17:128-135.
17. Sansare K, Raghav M, Mallya S, et al. Aggressive condylar resorption. *J Craniofac Surg*. 2013;24:E95-E96.
18. Hatcher DC. Progressive condylar resorption: pathologic processes and imaging considerations. *Semin Orthodont*. 2013;19: 97-105.
19. Mercuri LG. A rationale for total alloplastic temporomandibular joint reconstruction in the management of idiopathic/progressive condylar resorption. *J Oral Maxillofac Surg*. 2007;65:1600-1609.
20. Moore KE, Gooris PJ, Stoelinga PJ. The contributing role of condylar resorption to skeletal relapse following mandibular advancement surgery: report of five cases. *J Oral Maxillofac Surg*. 1991;49:448-460.
21. Hoppenreijs TJM, Stoelinga PJW, Grace KL, Robben CMG. Long-term evaluation of patients with progressive condylar resorption following orthognathic surgery. *Int J Oral Maxillofac Surg*. 2010;28:411-418.
22. Sansare K, Raghav M, Mallya SM, Karjodkar F. Management-related outcomes and radiographic findings of idiopathic condylar resorption: a systematic review. *Int J Oral Maxillofac Surg*. 2015;44:209-216.
23. Catherine Z, Breton P, Bouletreau P. Management of dentoskeletal deformity due to condylar resorption: literature review. *Oral Surg Oral Med Oral Pathol Oral Radiol*. 2016;121:126-132.
24. Kajii TS, Fujita T, Sakaguchi Y, Shimada K. Osseous changes of the mandibular condyle affect backward-rotation of the mandibular ramus in Angle Class II orthodontic patients with idiopathic condylar resorption of the temporomandibular joint. *Cranio*. 2018: 1-8.
25. Hwang SJ, Haers PE, Sailer HF. The role of a posteriorly inclined condylar neck in condylar resorption after orthognathic surgery. *J Craniomaxillofac Surg*. 2000;28:85-90.

Reprint requests:

Yue Xu
No.56 Lingyuan Xi Road
Guangzhou
Guangdong Province
PR China, 510055.
Kou9315@163.com